ELSEVIER

Polarization holography reveals the nature of the grating in polymers containing azo-dye

P.-A. Blanche [a,*], Ph.C. Lemaire [a], C. Maertens [b], P. Dubois [b,1], R. Jérôme [b]

[a] *Centre Spatial de Liège, Université de Liège, Parc Scientifique du Sart Tilman, Avenue du Pré-Aily, B-4031 Angleur-Liège, Belgium*
[b] *Center for Educational and Research on Macromolecules, Université de Liège, Sart Tilman B6a, B-4000 Liège, Belgium*

Abstract

To study the origin of reversible holographic recording in three polymers containing the same azo-dye, we have measured the diffraction efficiency and analyzed the gratings characteristics for various writing beams polarizations. The amplitude of the holographic grating, as well as the ratio between index and absorption modulations, have been investigated by gratings shifting. The total amount of diffracted power and the diffraction efficiency versus the reading beam polarization has been measured by non-degenerated four waves mixing. These experiments have revealed that the molecular mechanisms of holographic recording in the studied compounds are different. The photoinduced orientation of the chromophores is predominant for C6–C11–DMNPAA; so, in C11–C6–DMNPAA (DMNPAA: 2,5-dimethyl-4-(*p*-nitrophenylazo)anisole), the refractive index variation comes from the presence of both *trans* and *cis* populations generated by photoisomerization. The behavior of the PVK:DMNPAA is included between these extreme cases since both phenomena act. © 2000 Elsevier Science B.V. All rights reserved.

Keywords: Polymer; Holography; Molecular orientation; Photoinduced birefringence

1. Introduction

Polymers containing azo-dye are known since a long time for their possibilities of holographic recording [1,2]. The latter seems to be well understood and come from the reorientation or by *trans–cis* photoisomerization of the molecules by light polarization [3–5]. Molecular reorientation induces phenomena such as photoinduced birefringence, dichroism, and allows to write polarization holograms [5–11]. Since these properties are of significant interest for applications, azo-dye are currently intensively studied.

In a previous paper [11], we have analyzed the influence of the temperature on the photoinduced birefringence as well as on the holographic recording of three polymers containing the same azo-dye. Mathematical models have been developed in order to fit the transmitted and diffracted efficiency versus temperature measurements as well as to define parameters able to characterize the

* Corresponding author. Present address: Optical Sciences Center, University of Arizona, Tucson, AZ 85721, USA. Tel.: +1-520-621-2229; fax: +1-520-621-9610.

E-mail address: pablanche@optics.arizona.edu (P.-A. Blanche).

[1] Present address: SMPC, Université de Mons-Hainaut, B-7000 Mons, Belgium.

compounds. During this study, we have found that one of the three polymers (C11–C6–DMNPAA) (DMNPAA: 2,5-dimethyl-4-(*p*-nitrophenylazo)anisole) has a strange behavior facing both others and its efficiency cannot be fitted properly by our models. We have then postulated that the molecular behavior of the chromophores in this polymer could be different from the one previously expected. The present paper details our investigations to understand the molecular mechanisms taking place into these three polymers. The method used is polarization holography.

The three polymers synthesized are poly[*N*-vinyl carbazole] (PVK) doped with 15 weight percent (wt.%) of DMNPAA and plasticized with 30 wt.% of *N*-ethyl-carbazole (ECZ, the PVK monomer). Both others are copolymers constituted of [ω-(*N*-carbazolyl)alkylmethacrylate] and [4-(11-methacryloylalkyloxy)-2,5-dimethylphenyl](4-nitrophenyl)diazene where alkyl spacers length has been set to be hexyl and undecyl for the C6–C11–DMNPAA and undecyl and hexyl for the C11–C6–DMNPAA. The proportion of the copolymer is such that there is also 15 wt.% of azodye in these compounds. Their chemical structure is presented in Fig. 1. The glass transition temperatures (T_g) have been measured by differential scanning calorimetry to be 15°C for the PVK:DMNPAA, 56°C for the C6–C11–DMNPAA and −20°C for the C11–C6–DMNPAA. Polymers and chromophore synthesis can be found elsewhere [12].

PVK:DMNPAA polymer is well known for its photorefractive effect when a little amount of trinitrofluorenone sensitizer is added [13,14]. In our experiments, no photorefractive effect could be induced in the polymers since there is no sensitizer to form a charge transfer complex with the carbazole group present in the three compounds.

Samples have been made by pressing polymer powder between two glass plates heated around 20°C above the compound glass transition temperature. Thickness is determined by 70 μm spacers. No crystallization has been observed.

In polymers containing azo-dye, two mechanisms allow to write holograms: molecular reorientation and presence of both *trans* and *cis* isomer population. The fact that one or the other take
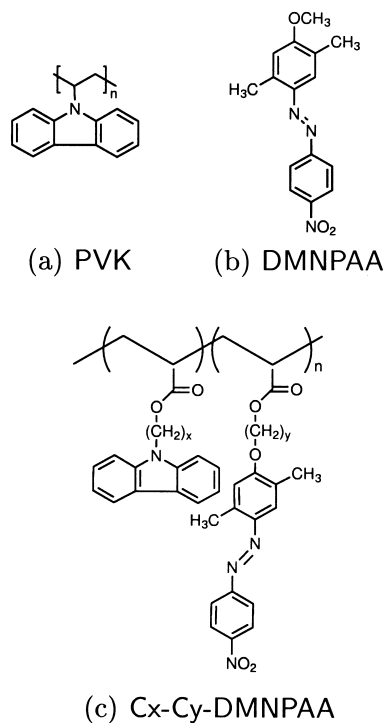

(a) PVK   (b) DMNPAA

(c) Cx-Cy-DMNPAA

Fig. 1. Molecular structure representation of the three compounds studied in the order of their acronym given ($n = 15$ wt.%).

place in the compound depend on the molecular time constants.

Molecular reorientation results of the combination of three processes: the selective *trans* to *cis* photoisomerization, the angular diffusion and the *cis* to *trans* relaxation [10,15–18]. We have plotted in Fig. 2 the angular distribution of both the ground and excited levels of the chromophores according to the process acting (Fig. 2 does not come from any calculation but are based on Dumont's model [17]). The excited level includes molecules that has absorbed a photon, they are either in the *cis* form or in another conformation (i.e. triplet state or photodecomposition). Molecules that have relaxed in the *trans* form but still having vibrational energy allowing them to rotate in the matrix are considered to be in the excited level. Thus, ground level only contains molecules that have not absorbed any photon since a certain time and have dissipated their vibrational energy.

At rest, all the molecules are in the ground level and the distribution is isotropic (Fig. 2(a)). When
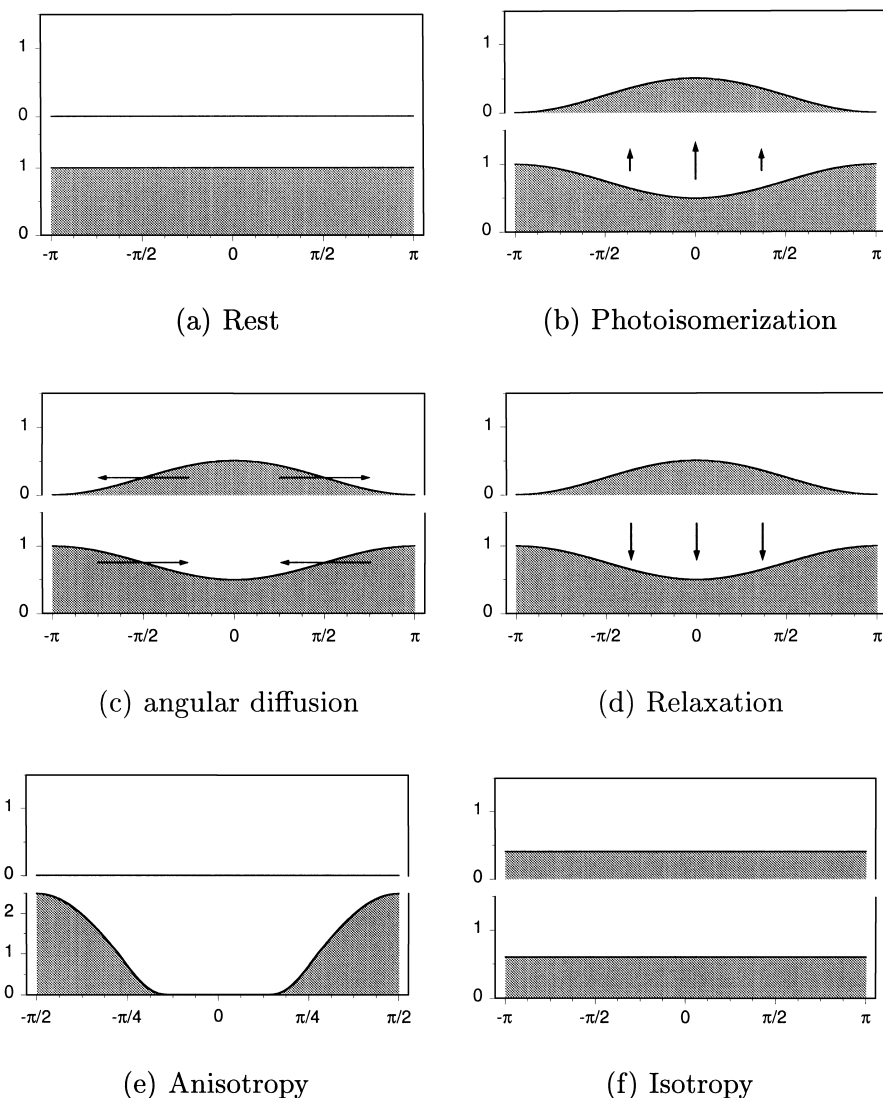
Fig. 2. Angular distribution of the ground and the excited levels illustrating the different mechanisms taking place during illumination of the chromophores with a linearly polarized light.

polarized beam is switched on, selective photo-isomerization begins and molecule oriented along the polarization axis (0°) are more likely pumped to the excited level. Levels become anisotropic (Fig. 2(b)). Angular diffusion is due to thermal agitation, it happens in both levels but at different rates due to the different molecular conformations. This mechanism tends to restore the isotropy broken by the optical pumping (Fig. 2(c)). *Cis–trans* relaxation occurs either by another photo-absorption or by thermal relaxation. Thermal relaxation is isotropic: the rate does not depend on the molecular orientation (Fig. 2(d)). Multiple cycles of these three mechanisms could lead to anisotropy of the molecular distribution. Indeed, if angular diffusion in ground state is slower than in excited state and slower than a excitation–relaxation cycle, this mechanism combined with multiple selective photoexcitation and isotropic relaxation modifies the angular distribution of the

molecules. Fig. 2(e) shows the distribution in such conditions when the polarized light has been switched off and the molecules have relaxed.

However, since the three above mentioned processes can have different time constants, an alternative mechanism can happen. If angular diffusion is much more faster than excitation and relaxation, angular distributions in both levels will be smoothed rapidly and no anisotropy will appear. The final distribution, presented in Fig. 2(f), will be isotropic. In these conditions, the refractive index can change since there is two molecular populations (*trans* and *cis*), but there will be no anisotropic phenomena such as birefringence and dichroism.

To put forward the molecular mechanisms, specific polarizations of the writing beams have been used to record holograms in the samples. These polarizations lead to various interference patterns that we have tried to represent graphically in Fig. 3, together with the polarization of the incident beams. The precise calculation of the patterns according to the incoming beams polarization as well as their incidence angle θ can be found in Ref. [19]. The definition and the utility of the selected configurations are the following:

VV $\forall \theta$ (Fig. 3(a)). Both incident beams are polarized linearly and their polarization vector is perpendicular to the incident plane. The interference pattern is modulated in intensity and constituted by linear polarizations oriented like the ones of the writing beams. This configuration will be used as a reference for the other polarizations.

HH $\theta \approx 0$ (Fig. 3(b)). Incoming beams are linearly polarized along the incident plane. The figure obtained is quite similar to the one of the VV case with polarization vectors turned at 90°. This configuration is useful to determine whether or not there is surface grating caused by polymer migration. Indeed, this kind of grating has already been shown in azo-dye doped polymers and their amplitude varies with the polarization orientation [2,20,21].

VH $\theta \approx 0$ (Fig. 3(c)). Incident beams are linearly polarized in perpendicular directions. So, one is along the plane of incidence and the other is perpendicular to this plane. The resulting interference pattern is the more complex. It is consti-
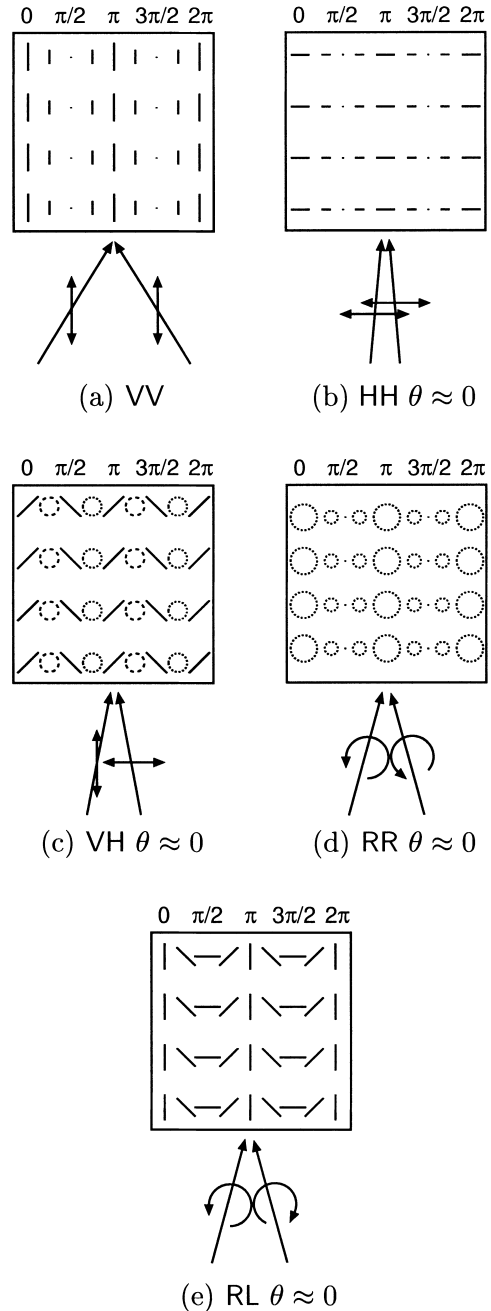

Fig. 3. Graphic representation of the interference patterns obtained for various polarization configurations of the incident beams. Different dashes represent left or right circular polarizations. Numbers on the top of the graphs are relative to the phase shift between the two incident waves. See text for more details.

tuted by linear polarizations oriented at 45° from those of incident beams, separated by left and the right circular polarizations. It has to be noted that there is no intensity modulation in this case. Linear polarizations will induce molecular orientation and/or presence of *cis* isomers according to the molecular ability since, circular polarizations do not produce any molecular orientation in the polarization plane and could only isomerize the chromophores isotropically.

RR $\theta \approx 0$ *(Fig. 3(d))*. Both incident beams are circularly polarized in the same direction (right in the present case). Pattern is modulated in intensity with circular polarizations oriented as the one of the incoming beams. Only few anisotropy could be produced by this pattern, but it can reveal presence of *trans* and *cis* populations.

RL $\theta \approx 0$ *(Fig. 3(e))*. One beam is right circularly polarized, the other is left circularly polarized. The interference pattern is only constituted by linear polarizations that turn with the beams phase. There is no intensity modulation. Isomerization is identical over all the pattern surface and so, cannot induce grating. However, anisotropy is produced along different axes. Only photoinduced orientation allows holographic recording with this configuration.

2. Grating characterization by two waves coupling

Two beams coming from an argon laser (514 nm), linearly or circularly polarized, cross each other in the sample to form an interference pattern. The latter is recorded by the polymer film as molecular modifications (isomerization or reorientation). By shifting the interference pattern according to the grating written into the sample, one obtains a modulation of the output beams intensity. Mathematical process allows to calculate the amplitude of the holographic grating, and to determine if there is an absorption or an index grating. It is also possible to calculate the phase shift between the recorded gratings and the interference pattern. This method which has been introduced by Sutter and Günter [22] and refined by Walch and Moerner [23] is really powerful since one can determine various parameters and detect gratings with very low diffraction efficiencies (i.e. 10^{-5}) due to the synchronous detection.

The setup used is presented in Fig. 4. The phase shifting requested between the written grating and the illumination pattern is produced by moving the mirror reflecting one of the laser beam. The incident angle of the laser beams is approximately 5°. Thus, we are in the conditions of small angles required for obtaining the interfering patterns described above ($\theta \approx 0$); but still in the Bragg regime since no other diffraction order is generated.

In order to not induce thermal grating or chemical degradation of the azo molecules, the intensity of the argon beams has been set at 1 mW/cm^2 [24]. Experiments have been done at ambient temperature.

Our setup geometry is fully symmetrical, i.e. both laser beams intensities are identical, their incidence angles are equal and the sample is perpendicular to the bisector of the angle formed by
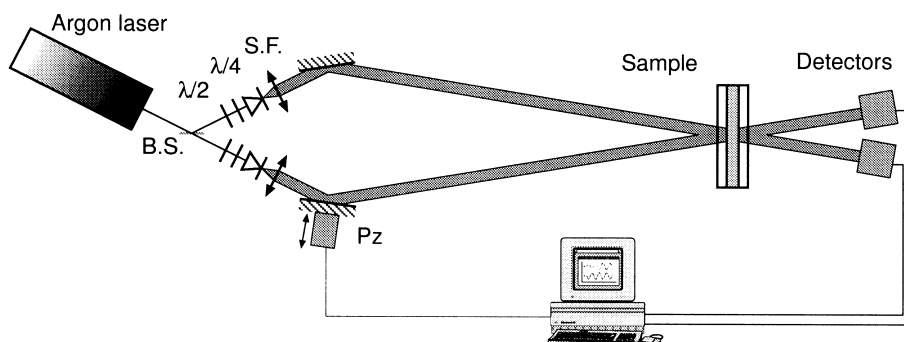

Fig. 4. Gratings shifting setup. B.S.: 50/50 beams splitter, S.F.: spatial filter, λ/x: retardation wave plate, Pz: piezoelectric transducer.

the beams. We are also in the Bragg regime. In these conditions, when the interference pattern is moved at the constant speed v along the sample plane, the intensities of the output beams are given by:

$$I_1 = I_0 \exp\left[-\frac{\alpha d}{\cos\theta}\right]\left[1 - 2Ad\cos\left(\varphi_A + \frac{2\pi vt}{\Lambda_G}\right)\right.$$

$$\left. + 2Pd\sin\left(\varphi_P + \frac{2\pi vt}{\Lambda_G}\right)\right], \tag{1a}$$

$$I_2 = I_0 \exp\left[-\frac{\alpha d}{\cos\theta}\right]\left[1 - 2Ad\cos\left(\varphi_A + \frac{2\pi vt}{\Lambda_G}\right)\right.$$

$$\left. - 2Pd\sin\left(\varphi_P + \frac{2\pi vt}{\Lambda_G}\right)\right], \tag{1b}$$

where I_0 is the incident intensity, α is the absorption coefficient of the sample, d is its thickness and Λ_G acts as the grating spacing. The $2\pi vt/\Lambda_G$ expression is the phase induced by the mirror displacement. A and P are, respectively, the diffraction amplitude of the absorption grating and of the index grating. They are defined by Eqs. (2a) and (2b)

$$A = \frac{\pi}{\lambda\cos\theta}\,\Delta\alpha, \tag{2a}$$

$$P = \frac{\pi}{\lambda\cos\theta}\,\Delta n, \tag{2b}$$

where λ is the reading wavelength, $\Delta\alpha$ the absorption modulation and Δn the refractive index modulation.

As it can be seen in Eqs. (1a) and (1b), the output beams intensity will oscillate with the grating shifting. In the case of a pure absorption grating, I_1 and I_2 will be in phase. For an index grating, they will be π phase shifted. When both gratings exist in the sample, the sum and the difference of I_1 and I_2 allow to calculate the amplitude (A and P) as well as the phase (φ_A and φ_P) of the gratings:

$$I^{(+)} = I_1 + I_2 = I_0 \exp\left(-\frac{\alpha d}{\cos\theta}\right)$$

$$\times \left[2 - 4Ad\cos\left(\varphi_A + \frac{2\pi vt}{\Lambda_G}\right)\right], \tag{3a}$$

$$I^{(-)} = I_1 - I_2 = I_0 \exp\left(-\frac{\alpha d}{\cos\theta}\right)$$

$$\times \left[0 + 4Pd\sin\left(\varphi_P + \frac{2\pi vt}{\Lambda_G}\right)\right]. \tag{3b}$$

2.1. Modulation amplitude

To perform the measurement, the interference pattern has been let a sufficiently long time (several minutes) to ensure the grating is fully recorded in the sample. The grating has been shifted at a speed much faster than the writing time of the hologram to be sure to not erase the latter. Displacement is done within a second. We have recorded the amplitude of the output beams modulation.

Geometrical factors as well as absorption coefficient of the sample are introduced in Eqs. (3a) and (3b), it is then difficult to determine the absolute amplitude of the holographic grating. Moreover, we do not need absolute measurement but only relative values to compare the various polarization configurations.

The graphics shown in Fig. 5 present normalized amplitude of the holographic grating according to five polarization configurations for the three polymers. We understand by the "amplitude of the holographic grating" the amplitude of the modulations recorded on the detectors, which is proportional to the grating amplitude if there is only one grating recorded in the material (see Eqs. (1a) and (1b)). From these measurements, conclusions are:

(1) Gratings amplitudes for the VV and HH configurations are identical for the three compounds studied. So, there is no surface grating written in these polymers. At least, in our experimental conditions (intensity and writing angle).

(2) The C6–C11–DMNPAA (Fig. 5(a)) shows a weak modulation in the RR configuration. The latter generates a pattern only constituted by circular polarizations (Fig. 3(d)). So, this configuration can only produce grating by changing the *cis:trans* population ratio, only minor orientational effects can happen. The fact that there is only very weak grating recorded in this configuration indicate that the holographic recording in
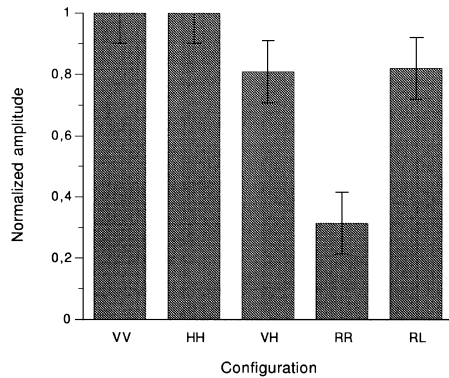
(a) C6-C11-DMNPAA
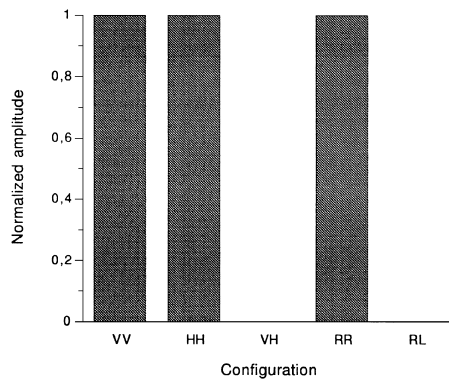
(b) C11-C6-DMNPAA
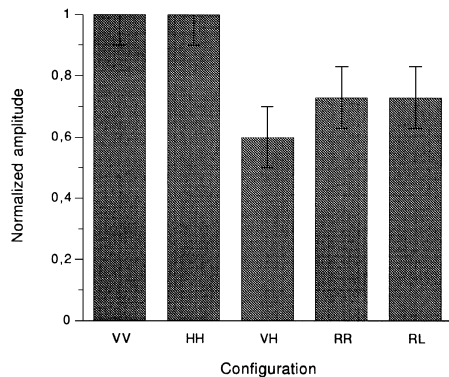
(c) PVK:DMNPAA

Fig. 5. Amplitude of the holographic grating according to the polarization configuration of the writing beams for the three compounds studied.

this polymer is driven mainly by the reorientation of the chromophores, exactly as expected.

(3) Conversely of the precedent case, for the C11–C6–DMNPAA sample (Fig. 5(b)), there must be an intensity modulation to record holograms. Indeed, the pure polarization patterns do not give any output modulation (configurations VH and RL). So, *there is no molecular reorientation in the C11–C6–DMNPAA*. The holographic recording certainly comes from the presence of both *trans* and *cis* populations that have different refractive indices.

(4) Concerning the PVK:DMNPAA (Fig. 5(c)), its behavior is intermediate. All configurations can be recorded with approximately the same amplitude. We believe there must be two recording mechanisms: one responsible of the modulation observed with the RR polarization; the other, inducing grating with orthogonally polarized writing beams.

2.2. Index and absorption gratings

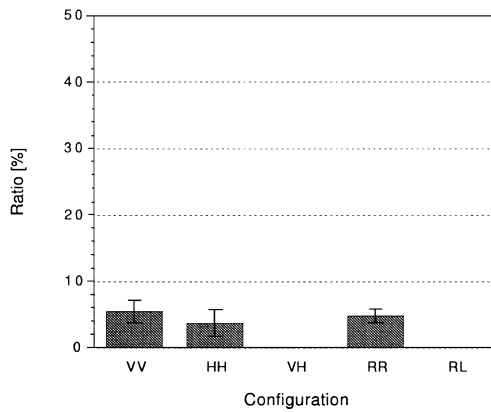In Fig. 6, the ratio between the amplitude of the absorption grating and the one of the index grating is plotted:

$$\frac{\Delta I^{(+)}}{\Delta I^{(-)}} = \frac{A}{P} . \tag{4}$$

One can see that, if the index modulation predominates for all the three compounds, there is an absorption component that is not negligible in various cases. The ratio between the gratings is quite similar for the VV, HH and RR configurations, those are the ones for which intensity modulation exists. For the VH and RL polarizations, there is a significant modification: the ratio increases for the C6–C11–DMNPAA and for the PVK:DMNPAA since, there is no grating (so no ratio) for the C11–C6–DMNPAA (see Section 2.1).

The PVK:DMNPAA case is very interesting since it brings information on the imaginary part of the *trans* and *cis* dipolar moments ($\Im\mu$). RR configuration induces very weak absorption grating. Now, predominant recording mechanism in this configuration is isomerization. So, one can conclude that $\Im\mu$ of the *cis* form is quite the same than the mean of the *trans* form. At the opposite, since in VH and RL configurations absorption
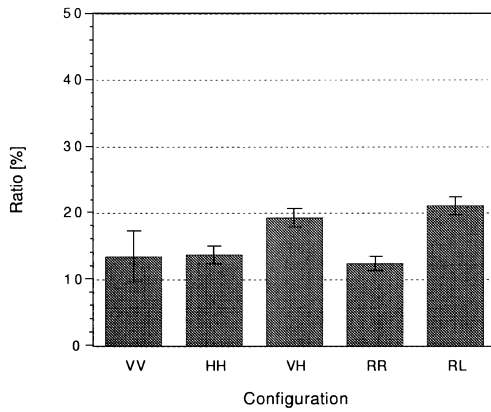
(a) C6-C11-DMNPAA

(b) C11-C6-DMNPAA
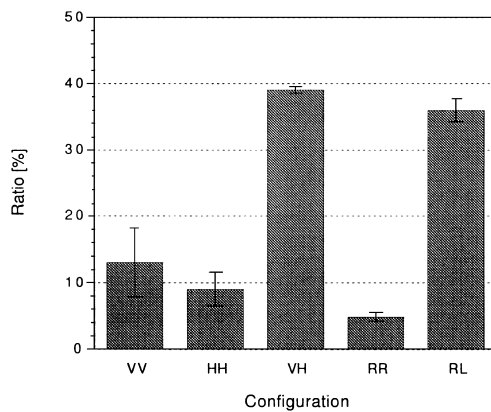
(c) PVK:DMNPAA

Fig. 6. Ratio between the amplitudes of the absorption and the index gratings for five polarization configurations of the incident beams.

gratings are more important, and these polarizations favor chromophore orientation, one can say that longitudinal and transversal $\Im\mu$ of the *trans* isomers are very different. This can also be noted by comparing the C6–C11–DMNPAA and the C11–C6–DMNPAA. For the latter, precedent experiment has shown that there is no molecular orientation, and there is only few absorption grating. So, *trans* and *cis* mean $\Im\mu$ are similar. For the C6–C11–DMNPAA, the absorption grating is more predominant and chromophores reorientation has been observed. DMNPAA perpendicular and parallel *trans* $\Im\mu$ are different.

No temporal modification of the ratio between the gratings amplitude has to be mentioned. Thus, for a given compound, the phenomena responsible of the index and the absorption variations have the same time constants and, more likely, come from the same mechanism.

We have not measured any phase shifting between the recorded gratings and the illumination pattern: $\varphi_A = \varphi_P = 0$ or π. Both are local. For all the compounds, $\varphi_A = \pi$ since the movement of the interference pattern decreases the total output intensity ($I^{(+)}$). So, the absorption grating is due to photobleaching of the polymer.

3. Diffraction efficiency measurement

Measurements of the diffraction efficiency according to the various interference patterns as well as the polarization angle of the reading beam have been carried out. The experimental setup is presented in Fig. 7. Exactly the same writing beams geometry has been reused from the phase shifting experiments. The hologram is read in situ by means of a linearly polarized helium–neon laser beam (633 nm). Its polarization axis can be turned by means of a polarizer, in order to determine if the holographic grating written is isotropic or not. The incident angle of the HeNe beam is equal to the Bragg angle.

We have plotted, in Fig. 8, the normalized diffraction efficiency of the HeNe beam according to its polarization angle; this for the five interference patterns. For each graphs, the diffracted intensity has been normalized to its highest value. The
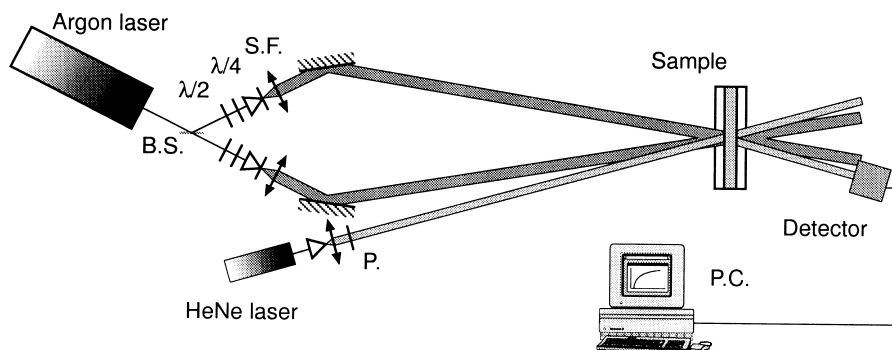
Fig. 7. Experimental setup used to measure the diffraction efficiency according to the polarization of the writing and reading beams. B.S.: 50/50 beams splitter, S.F.: spatial filter, λ/x: retardation wave plate, P: polarizer.

maximum diffraction efficiency measured is 3.8×10^{-2} for the C6–C11–DMNPAA, 6.8×10^{-4} for the C11–C6–DMNPAA and 1.34×10^{-3} for the PVK:DMNPAA.

The comparison of the three graphics presented in Fig. 8 shows that the behavior of the diffraction efficiency, according to the polarization configuration, is very different from one compound to another. However, we can distinguish the own characteristics of the interference patterns: the diffraction efficiency is modulated according to a sine square for the HH and the VV configurations in a symmetrical way; then, the diffracted amplitude is constant for the VH, RR and RL incident polarizations. These properties come directly from the polarization symmetry of the interference patterns that can be remarked at Fig. 3.

Specific information can be extracted by analyzing the ratio of the diffracted intensity at $0°$ and $90°$ in the VV and HH configurations. Indeed, if the molecular orientation is the only acting mechanism, we know that parallel to the writing beam polarization, there is a depletion in the *trans* angular distribution and thus a large modulation of the holographic grating. Instead, in the orthogonal direction, chromophore can be oriented randomly in the plane defined by the propagation beams direction. The grating modulation is considerably reduced. The ratio between both diffracted intensities at $0°$ and $90°$ polarizations is important. That is what appears in the Fig. 8(a): for the C6–C11–DMNPAA compound, the diffraction efficiency falls practically to zero when writing and reading polarizations are orthogonal.

When it is the presence of both *trans* and *cis* populations that characterize the holographic grating, the following reasoning can be done: in the illuminated zones of the interference pattern, the *cis* isomers are present and their dipolar moments is quite homogeneous; then, in the dark areas, *trans* isomers are randomly distributed. The hologram is so more isotropic in polarization compared to what we have for the molecular reorientation. Meanwhile, it must be noted that the *trans* to *cis* isomerization is still selective and so, the angular distribution of the *trans* molecules is not homogeneous. This explains the remaining anisotropy. It is exactly what is observed for the C11–C6–DMNPAA, where the curves VV and HH of Fig. 8(b) are only weakly modulated.

Once again, the case of the PVK:DMNPAA compound is intermediate, since the diffracted intensity ratio is around 40%. We can conclude that both recording mechanisms are present: reorientation induced anisotropy but *trans* and *cis* distributions are also smoothed by diffusion.

To analyze the diffraction efficiency for each polymer, it is also convenient to plot the total amount of diffracted energy. This can be calculated by integrating the diffraction efficiency over the angles of the reading beam polarization $(0–\pi)$, or by performing the diffraction efficiency experiments with an unpolarized reading beam. In Fig. 9, this quantity has been normalized, for each polymer, to the maximum value obtained.
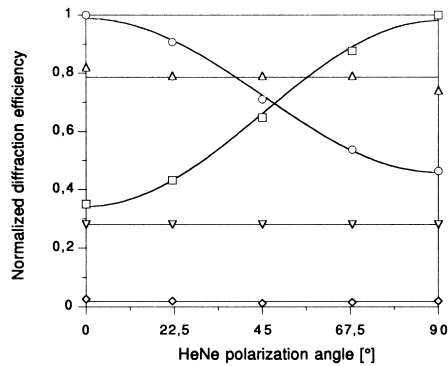
Fig. 9(a) shows that, for the C6–C11–DMNPAA, the diffraction efficiency in the configuration RL is higher than for the other cases.
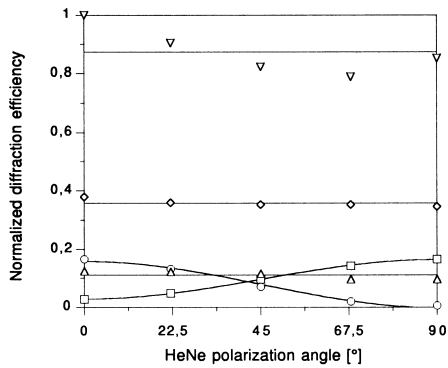
(a) C6-C11-DMNPAA
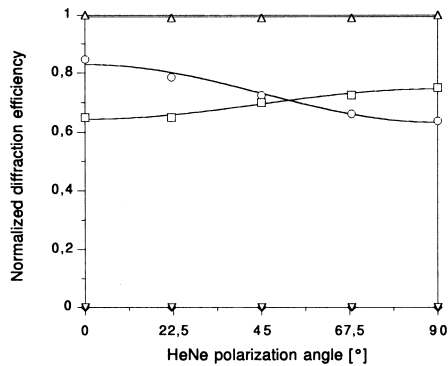
(b) C11-C6-DMNPAA

(c) PVK:DMNPAA
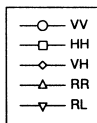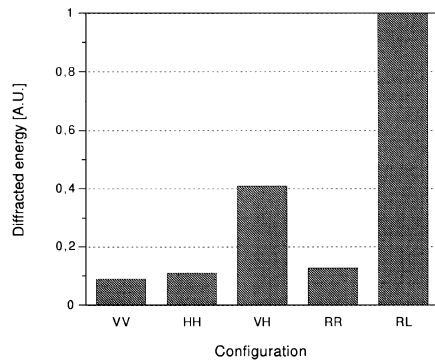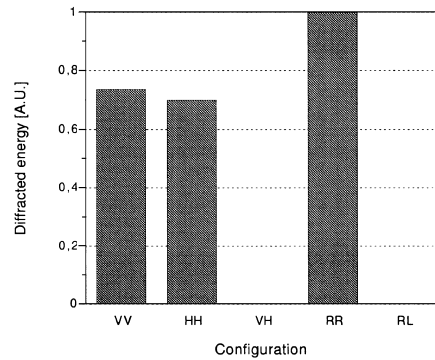
Caption

○—— VV
□—— HH
◇—— VH
△—— RR
▽—— RL

Fig. 8. Diffraction efficiency of the HeNe beam according to its polarization angle and, for different polarization configurations of the writing beams.

(a) C6-C11-DMNPAA

(b) C11-C6-DMNPAA
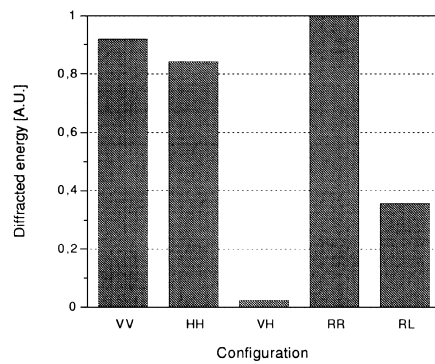
(c) PVK:DMNPAA

Fig. 9. Total amount of energy diffracted according to the polarization of the writing beams.

This is due to the fact that the interference pattern for these writing polarizations is constituted by linear polarizations with axes turn according to the phase (Fig. 3(e)). This is the more efficient configuration for molecular reorientation since the

latter takes place in all the holographic area. It should be noted that, in the VH mode, since polarizations at $\pi/2$ and $3\pi/2$ are circular, the index modulation is not necessary sinusoidal and diffraction is then reduced.

In the case of the C11–C6–DMNPAA (Fig. 9(b)), one can see that the diffraction efficiency increases in the RR configuration compared to the VV and HH states. This polymer shows only isomerization; the more efficient configuration is then obtained when the polarization of the interference pattern is circular (RR configuration). Indeed, isomerization *trans–cis* is realized isotropically in all the directions of the polarization plan. In the case of linear polarizations (VV and HH), molecules placed perpendicularly do not undergo the light electric field influence.

For the PVK:DMNPAA (Fig. 9(c)), the diffraction efficiency in VH configuration is an order of magnitude lower than in the other cases. This can be interpreted as follows: since there are molecular reorientation (because there is diffraction in RL case) and isomerization (since there is diffraction in RR case), the VH interference pattern in this compound induces some reorientation of the chromophores where the polarizations are linear and some isomerization where the polarizations are circular (see Fig. 3(d)). Both gratings overlay and cancel their effects.

We have just seen that the molecular mechanisms of holographic recording can perfectly explain the different behaviors of diffraction efficiency observed according to the writing polarizations.

4. Conclusions

Phase shifting and the diffraction efficiency experiments, realized according to various polarization of the writing beams, have shown, in a self-reliant way, that the holographic recording process into the three compounds C6–C11–DMNPAA, C11–C6–DMNPAA and PVK:DMNPAA is different although they contain the same chromophore. We have found that:

(1) For the C6–C11–DMNPAA, the photoinduced reorientation of the azo-dye molecules acts for the major part in the holographic recording process. The presence of *cis* isomers population only plays a minor role. This is the well known holographic recording process for azo-dye doped polymers.

(2) In an opposite way, the C11–C6–DMNPAA compound does not show any molecular reorientation, and the anisotropy is very weak. Holograms recording comes from the isomerization of the chromophores. This is the presence of both *trans* and *cis* isomer populations that induces index change. This explains why we have previously observed so many discrepancies between the photoinduced birefringence and the diffraction efficiency for this polymer [11].

(3) The analysis of the PVK:DMNPAA polymers is really interesting. It reveals an ''intermediary'' behavior: the presence of *cis* isomers is as important as the molecular reorientation of the *trans* form for the holographic recording.

The comparison of these results lets us think that the different behaviors observed are due to the different glass transition temperatures (T_g) of the compounds. Indeed, we have discussed in the introduction the two extreme cases that can be observed: photoinduced anisotropy and photoinduced isomerization. They can both be explained by the three same mechanisms: excitation, diffusion and relaxation but with different time constants. Thus, for the C6–C11–DMNPAA, whose T_g is above the ambient temperature, the angular diffusion due to thermal agitation is low compared to isomerization and relaxation; molecules can then be aligned by the light, what leads to photoinduced anisotropy. The T_g of the C11–C6–DMNPAA is under the ambient temperature and the thermal agitation can easily randomize the molecular distribution. So, diffusion is faster than excitation and/or relaxation and smoothes the angular anisotropy of the levels (see Fig. 2(c)). Only the effects of the populations are observable. For the PVK:DMNPAA whose T_g is near the ambient temperature, diffusion also smoothes the distribution but not fast enough, anisotropy stays observable and both mechanisms can be detected.

We have shown that the T_g influences much more the chromophores behavior than the chemical link between the dye and the polymer main

chain. The temporal analysis of multi-wavelengths dichroism has confirmed all these conclusions [10].

References

[1] C.M. Verber, R.E. Schwerzel, P.J. Perry, R.A. Craig, Holographic recording materials development, Technical Report No. NASA-CR-144991, National Aeronautics and Space Administration, 1976; reproduction: N76-23544 National Technical Information Service, Springfield, VA, USA.

[2] P.S. Ramanujam, N.C.R. Holme, L. Nikolova, R.H. Berg, S. Hvilsted, E.T. Kristensen, C. Kulinna, A.B. Nielsen, M. Pedersen, Erasable holographic storage in azobenzene polyesters and peptides, in: S.A. Benton, T. Trout (Eds.), Practical Holography XI and Holographic Material III, SPIE Proceedings, vol. 3011, San Jose, 1997, pp. 319–326.

[3] A.M. Makushenko, B.S. Neporent, O.V. Stolbova, Reversible orientation photodichroism and photoisomerization of aromatic azo compounds I: model of the system, Optical Spectroscopy (USSR) 31 (1971) 295–299.

[4] G.S. Kumar, D.C. Neckers, Photochemistry of azobenzene-containing polymers, Chemical Review 89 (1989) 1915–1925.

[5] P.-A. Blanche, Ph.C. Lemaire, C. Maertens, P. Dubois, R. Jérôme, Polarised light induced birefringence in azo dye doped polymer: a new model and polarised holographic experiments, Optics Communication 139 (1997) 92–98.

[6] T. Todorov, L. Nikolova, N. Tomova, Polarization holography. 1: a new high-efficiency organic material with reversible photoinduced birefringence, Applied Optics 23 (1984) 4309–4312.

[7] S. Calixto, R.A. Lessard, Holographic recording and reconstruction of polarized light with dyed plastic, Applied Optics 23 (1984) 4313–4318.

[8] L. Nikolova, T. Todorov, M. Ivanov, F. Andruzzi, S. Hvilster, P.S. Ramanujam, Polarization holographic gratings in side-chain azobenzene polyesters with linear and circular photoanisotropy, Applied Optics 35 (1996) 3835–3840.

[9] C. Wang, H. Fei, Y. Yang, Z. Wei, Y. Qiu, Y. Chen, Photoinduced anisotropy and polarization holography in azobenzene side-chain polymer, Optics Communication 159 (1999) 58–62.

[10] P.-A. Blanche, Ph.C. Lemaire, M. Dumont, M. Fischer, Photoinduced orientation of azo dye in various polymers matrices, Optics Letters 24 (1999) 1349–1351.

[11] P.-A. Blanche, Ph.C. Lemaire, C. Maertens, P. Dubois, R. Jérôme, Photoinduced birefringence and diffraction efficiency in azo dye doped or grafted polymers: theory versus experiment of the temperature influence, Journal of Optical Society of America B 17 (2000) 729–740.

[12] C. Maertens, P. Dubois, R. Jérôme, P.-A. Blanche, Ph.C. Lemaire, Synthesis and polarized light induced birefringence of new polymethacrylates containing carbazolyl and azobenzene pendant groups, Journal of Polymer Science Part B: Polymer Physics 38 (2000) 205–213.

[13] B. Kippelen, N. Peyghambarian, S.R. Lyon, A.B. Padias, H.K. Hall Jr., New highly efficient photorefractive polymer composite for optical storage and image-processing applications, Electronics Letters 29 (1993) 1873–1874.

[14] K. Meerholz, B.L. Volodin, Sandalphon, B. Kippelen, N. Peyghambarian, A Photorefractive polymer with high optical gain and diffraction efficiency near 100%, Nature 371 (1994) 497–500.

[15] S. Morino, S. Machida, T. Yamashita, K. Horie, Photoinduced refractive index change and birefringence in poly(methyl methacrylate) containing *p*-(dimethylamino)azobenzene, Journal of Physical Chemistry 99 (1995) 10280–10284 and references therein.

[16] M. Dumont, A common model for optical ordering of photoisomerizable molecules, in: F. Kajzar, V.M. Agranovich, C.Y.-C. Lee (Eds.), Photorefractive Organic Materials. Science and Applications, High Technology, vol. 3, NATO Advanced Sciences Institutes Series, vol. 9, Kluwer, Dordrecht, 1996, pp. 501–511.

[17] M. Dumont, A general model for optically induced molecular order in amorphous materials via photoisomerization, Nonlinear Optics 15 (1996) 69–72.

[18] S. Hosotte, M. Dumont, Photoassisted poling and orientational relaxation of dye molecules in polymers. the case of spiropyran, in: G.R. Möhlmann (Ed.), Nonlinear Optical Properties of Organic Materials IX, SPIE Proceedings, vol. 2852, Denver, Colorado, 1996, pp. 53–63.

[19] T. Huang, K.H. Wagner, Coupled mode analysis of polarization volume hologram, IEEE Journal of Quantum Electronics 31 (1995) 372–390.

[20] P. Lefin, C. Fiorini, J.-M. Nunzi, Anisotropy of the photoinduced translation diffusion of azo-dyes, Optical Materials 9 (1998) 323–328.

[21] N.C.R. Holme, L. Nikolova, P.S. Ramanujam, S. Hvilsted, An analysis of the anisotropic and topographic gratings in a side-chain liquid crystalline azobenzene polyester, Applied Physics Letters 70 (1997) 1518–1520.

[22] K. Sutter, P. Günter, Photorefractive grating in organic crystal 2-cyclooctylamino-5-nitropyridine doped with 7,7,8,8-tetracyano-quinodimethane, Journal of the Optical Society of America B 7 (1990) 2274.

[23] C.A. Walsh, W.E. Moerner, Two-beam coupling measurements of grating phase in a photorefractive polymer, Journal of the Optical Society of America B 9 (1992) 1642–1647 + erratum.

[24] P.-A. Blanche, Ph.C. Lemaire, C. Maertens, P. Dubois, R. Jérôme, Limiting factor of the diffraction efficiency in azo dye doped polymers, in: R.A. Lessard (Ed.), Photopolymer Device Physics, Chemistry, and Applications IV, SPIE Proceedings, vol. 3417, Québec City, Québec, Canada, 1998.